

# Conductivity-model Parameterization for the Effect of Non-electrified Clouds to the Global Electric Circuit

Andreas J.G. Baumgaertner<sup>1\*</sup>, Greg M. Lucas<sup>1</sup>, Jeffrey P. Thayer<sup>1</sup>, and Sotirios A. Mallios<sup>2</sup>

<sup>1</sup>Aerospace Engineering Sciences Department, University of Colorado, Boulder, USA

<sup>2</sup>Department of Electrical Engineering, Pennsylvania State University, University Park, USA

**ABSTRACT:** It is well known that non-electrified clouds have a lower conductivity than the surrounding air, and therefore account for a significant fraction of the total resistance of the fair-weather part of the Global Electric Circuit. To quantify this, high-resolution GEC model simulations are performed. The results show that currents partially flow around non-electrified clouds, reducing their importance for fair-weather resistance. In global circulation model simulations of conductivity, information about cloud coverage is generally only available as “cloud cover fraction” for every model layer, and therefore cannot directly take into account the effect. Therefore, a parameterization for this effect is presented. An implementation for the conductivity simulations with CESM1(WACCM) is described, and the effects on the column resistance distributions as well as on total resistance are discussed.

## INTRODUCTION

Atmospheric electrical conductivity (the inverse of resistivity) largely determines the fair-weather current distribution and global resistance. Detailed descriptions of conductivity are provided by *Baumgaertner et al.* [2013], B13 hereafter, *Tinsley and Zhou* [2006], *Rycroft et al.* [2008], and *Zhou and Tinsley* [2010], ZT10 hereafter. Non-electrified clouds in the fair-weather region, i.e. clouds that do not contribute to the source current of the GEC, in general reduce conductivity, because cloud water droplets absorb ions [*Pruppacher and Klett*, 1997]. The effects can be quantified based on their ice and liquid droplet number concentrations and radii, see e.g. ZT10.

Non-electrified clouds have only been studied by a small number of authors. ZT10 were the first to include and parametrize these clouds in global calculations of conductivity and resistance. They suggested a reduction of conductivity between one and two orders of magnitude inside the cloud. However, as shown in the full discussion [*Baumgaertner et al.*, 2014, B14 hereafter] of the work presented here, their global treatment of clouds only holds for very small cirrus clouds and underestimates the resistance increase through clouds significantly. *Nicoll and Harrison* [2009] presented air-to-earth current density measurements from two sites in the United Kingdom, together with solar radiation measurements, and showed that current density below the cloud can be reduced, depending on cloud height and cloud thickness.

From conductivity, column resistance and global resistance can be derived, which are both important parameters for the GEC. Note however that the concept of column resistance is based on the assumption of small horizontal gradients in potential and conductivity, i.e. only vertically flowing currents. Strong horizontal gradients in potential and conductivity violate this approach, as will be demonstrated in the next section. Column resistance is classically defined as the vertical integration of the reciprocal of conductivity:

$$R_{col} = \int_{\text{surface}}^{\text{ionosphere}} \frac{1}{\sigma(z)} dz, \quad (1)$$

where  $dz$  are the layer thicknesses.

---

\*Corresponding author, email: work@andreas-baumgaertner.net, Postal address: Aerospace Engineering Sciences Department, University of Colorado, Boulder, CO 80309, USA

Then, global resistance is calculated as the horizontal integral of reciprocal column resistance:

$$R_{tot}^{col} = \left( \iint \frac{r^2 \cos(\lambda) d\phi d\lambda}{R_{col}(\phi, \lambda)} \right)^{-1}, \quad (2)$$

where  $r$  is the Earth's radius,  $\phi$  is longitude and  $\lambda$  is latitude.

For small clouds, where currents flow around the cloud as will be shown below, horizontal currents arise, and make the above approach invalid, and global resistance must be derived from Ohm's law by calculating the current flowing over a boundary with a fixed potential,

$$R_{tot}^{Ohm} = \frac{\Phi_I}{I_{tot}} \quad (3)$$

where  $\Phi_I$  is the ionospheric potential and  $I_{tot}$  the total GEC current, which can be calculated as the surface integral of the downward component of the air-to-earth current densities:

$$I_{tot} = \iint J_{\downarrow \text{air-to-earth}}(\phi, \lambda) r^2 \cos(\lambda) d\phi d\lambda. \quad (4)$$

Ionospheric potential,  $\Phi_I$ , and current density,  $J$ , can only be calculated by solving the Poisson type partial differential equation (PDE) for the GEC (see below). However, global 3-D models of the GEC are generally not employed on spatial resolutions that resolve clouds. Therefore, an approach is presented here that is based on replacing column resistance by an "effective column resistance"  $\hat{R}_{col}$ ,

$$\hat{R}_{col}(\phi, \lambda) = \frac{\Phi_I}{J_{\downarrow \text{air-to-earth}}(\phi, \lambda)} \quad (5)$$

which yields  $R_{tot}^{Ohm}$  when integrated horizontally.

## MODEL DESCRIPTIONS

### *GEC model*

For a given charge distribution  $S$ , determined by thunderstorms and electrified clouds, Gauss' law

$$\nabla \cdot \sigma E = S \quad (6)$$

relates the sources  $S$  with the electric field  $E$  for a lossy medium with conductivity  $\sigma$ . In the absence of magnetic fields, the electric field is the gradient of a potential  $\Phi$ :

$$E = -\nabla \Phi. \quad (7)$$

Substituting eq. 7 into eq. 6 yields the elliptical Poisson type PDE for the static GEC:

$$-\nabla \cdot [\sigma \nabla \Phi] = S. \quad (8)$$

The solution  $\Phi$  also yields the current density distribution  $J = -\sigma \nabla \Phi$ . For the GEC cloud simulations presented in the next section we specify a fixed ionospheric potential (Dirichlet boundary condition) of 300 kV at 60 km, and the earth's potential is set to zero. Also, the sources  $S$  are set to be zero. This formulation was implemented in the Fenics Python program [Logg *et al.*, 2012] to obtain the potential and current distribution throughout the domain using a finite element model formulation.

### Conductivity model

Conductivity calculations are performed using the Whole Atmosphere Community Climate model [Marsh *et al.*, 2013] which is part of the Community Earth System Model, CESM1(WACCM), with an additional module to calculate conductivity. The driving parameters in the conductivity module are temperature, density, pressure, aerosol concentrations, and cloud coverage. The model is described and evaluated in detail within B13, using average atmospheric and solar conditions. Here, we use Specified Dynamics version of WACCM (SD-WACCM), where temperatures and winds are nudged to meteorological assimilation analysis results (GEOS5), see Lamarque *et al.* [2012] for a description.

### SINGLE CLOUDS

For the GEC simulations, an average background (cloud-free) conductivity profile from the work by B13 is used with no horizontal variability. To simulate the effect of a single cloud, conductivity is reduced inside the cloud by a factor  $\eta=1/50$  after Zhou and Tinsley [2010].

Figure 1 presents (a) the current density distribution, (b) air-to-earth current densities, and (c) column resistances for a simulation of a cirrus cloud with a diameter of 10 km, a thickness of 1.5 km, spanning from 8 to 9.5 km. The top panel depicts the current streamlines with total current density. As expected, there is a strong reduction from an average current density of  $2.5 \text{ pA/m}^2$  to  $0.6 \text{ pA/m}^2$  inside the cloud. However, the streamlines show that currents bend around the cloud, leading to higher-than-average currents (red) at the edges. There is a current divergence above the cloud, and convergence below. The effect on the air-to-earth current density is shown in panel (b). The red line depicts the air-to-earth current densities if only vertical currents were permitted, i.e. the ionospheric potential divided by the column resistance  $R_{col}$ . The blue line shows the model result, indicating that the current density reduction is in fact less severe, but spread out several kilometers past the cloud edge. In panel (c), showing column resistance, the red line depicts the vertically integrated column resistance  $R_{col}$ , and the blue line depicts the column resistance  $\hat{R}_{col}$  calculated as ionospheric potential divided by simulated air-to-earth current density, as defined in Eq. 5.

In order to simplify further studies of cloud effects on larger horizontal domains, it is desirable to replace  $\hat{R}_{col}$  with only one value for the cloud area, where the fair-weather column resistance remains unchanged. Therefore, we are looking for a new cloud column resistance value  $\hat{R}_{col}^{cloud}$ , that takes into account the partial current flow around the cloud.

It is also possible to formulate this using current density, where the air-to-earth current density is replaced with a fair-weather current density, and a cloud current density  $\hat{J}_{air-to-earth}^{cloud}$ , because then

$$\hat{R}_{col}^{cloud} = \frac{\Phi}{\hat{J}_{air-to-earth}^{cloud}}. \quad (9)$$

The approach is depicted in Fig. 1b). By integrating  $J_{air-to-earth}^{no-cloud} - J_{air-to-earth}$  over the shown domain, i.e. the difference between the blue line and the fair-weather current density (green and blue areas), and dividing only by the area of the cloud, the current density reduction is attributed to the cloud area (indicated by arrows). So we define the cloud current density  $\hat{J}_{air-to-earth}^{cloud}$  as

$$\hat{J}_{air-to-earth}^{cloud} = J_{air-to-earth}^{no-cloud} - A^{-1} \iint \left( J_{air-to-earth}^{no-cloud} - J_{air-to-earth}(\phi, \lambda) \right) d\phi d\lambda \quad (10)$$

where  $A$  is the area of the cloud. The resulting current density is shown as the green line in Fig. 1b).

The green line in panel (c) of Fig. 1 shows the resulting column resistance  $\hat{R}_{col}^{cloud}$  using eq. 9. This is the average cloud column resistance while accounting for the off-vertical currents.

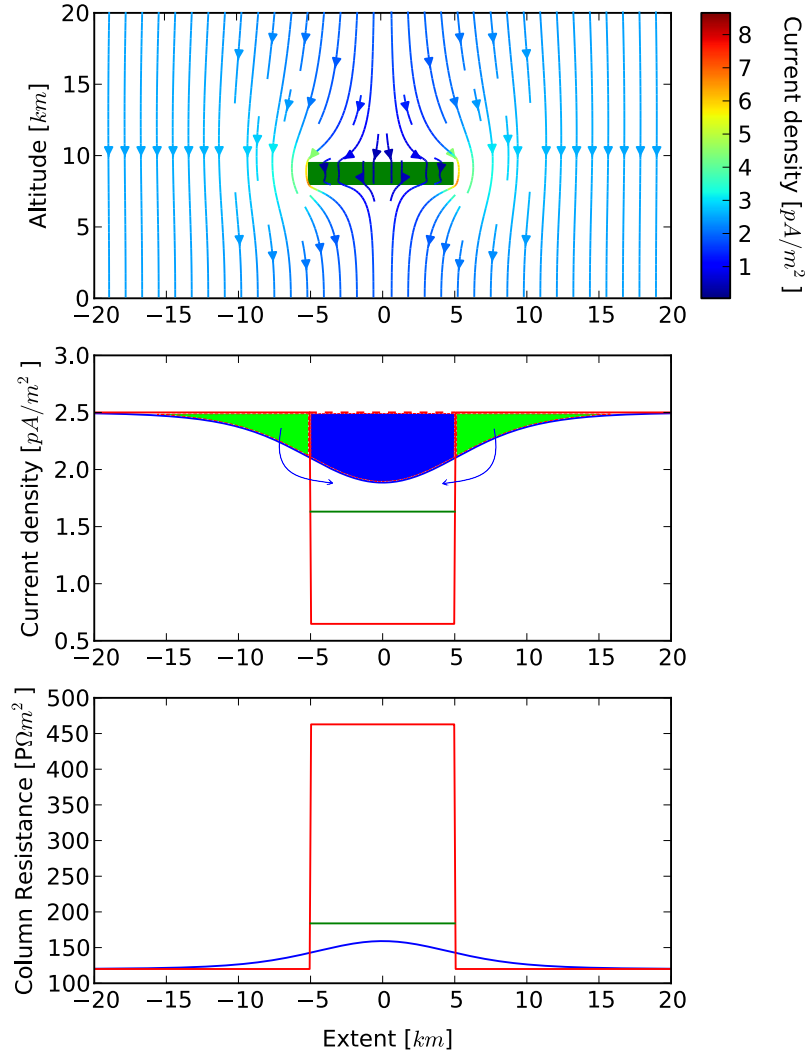


Figure 1: (a) current streamlines and total current density around a cirrus cloud (indicated by the green box) with a diameter of 10 km, located between 8 and 9.5 km altitude. (b) Model air-to-earth current density (blue), restricted to vertical currents only (red). (c) Effective column resistance  $\hat{R}_{col}$  (blue), column resistance for considering vertical currents only  $R_{col}$  (red), and mean effective cloud column resistance  $\hat{R}_{col}^{cloud}$  (green).

It is important to note that the derived column resistance values are independent of the ionospheric potential, and of the vertical and horizontal resolution of the simulation, as long as the cloud and the region below the cloud are resolved.

To compare the current divergence/convergence effect for different cloud types and horizontal dimensions, we compute the ratio  $\hat{R}_{col}^{cloud}/R_{col}^{cloud}$ , shown in Fig. 2, as a function of cloud diameter for a variety of cloud types. Here, cloud types are only distinguished by their altitude regime. From Fig. 2, one can see the effect is most important for clouds with a diameter less than 100 km. In the transition range, between 2 and 100 km, generally the effect is more pronounced, i.e. a smaller  $\hat{R}_{col}^{cloud}/R_{col}^{cloud}$ , for clouds with a high cloud bottom for which the current divergence/convergence becomes more important.

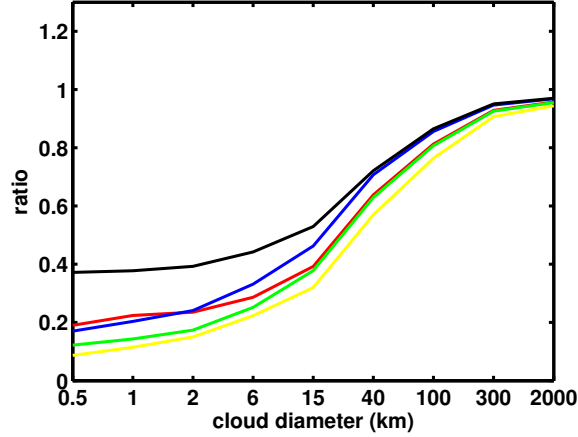


Figure 2: Horizontal-size dependence of  $\hat{R}_{col}^{cloud} / R_{col}^{cloud}$  for different altitudes of clouds: cumulus and stratocumulus (1–2 km, red), altostratus (3–5 km, green), altocumulus (2–3 km, blue), nimbostratus (2–5 km, yellow), cirrus (8–9.5 km, black).

The only available measurements of air-to-earth current density depending on cloud coverage were presented by *Nicoll and Harrison* [2009]. The authors found little change in the current density measurements, only fully-overcast conditions with thick clouds led to current density reductions. The model simulations support and explain these findings. Unfortunately, the authors did not present their results as a function of cloud size, since such data was not available, so a quantitative comparison or evaluation of the model results is not possible.

## GLOBAL EFFECT

For estimating the impact of non-electrified clouds on global resistance, it is necessary to take into account the cloud size distribution. *Wood and Field* [2011] have used MODIS, airplane and model data to show that the cloud chord length as well as the projected area obey a power law. For the cloud cover contribution  $C$  from clouds larger than  $x/x_{max}$  they showed that  $C(x) = 1 - (x/2000 \text{ km})^{0.3}$ . If we assume this result to be true individually for all types of clouds, the size-dependent cloud cover fraction is then  $g(h_i, type) = f(type) \cdot C_h(h_i)$  for cloud horizontal sizes  $h_i$ , where cloud-cover fraction  $f$  is given by satellite observations or model simulations.

The high-resolution simulations for single clouds in the previous section are used to derive the ratio  $\hat{R}_{col}^{cloud} / R_{col}^{no-cloud}$  for every cloud type. The column resistance  $\tilde{R}_{col}$  for a partially cloud-covered column can then be calculated by averaging the individual values for  $\hat{R}_{col}^{cloud}(h_i, type)$  weighted by the corresponding cloud cover fraction:

$$\tilde{R}_{col} = \left( \sum_{i,type} \left( \hat{R}_{col}^{cloud}(h_i, type) \right)^{-1} \cdot g(h_i, type) + \left( R_{col}^{no-cloud} \right)^{-1} \cdot \left( 1 - \sum_{i,type} g(h_i, type) \right) \right)^{-1}. \quad (11)$$

The Earth System Model CESM1(WACCM) was used to calculate column and global resistances, using the model cloud cover, which is provided as a function of altitude and horizontal location. The annual mean column resistances are shown in Fig. 3. The cloud-free atmosphere total resistance of  $165 \Omega$  increases by 73% to  $285 \Omega$ . If the current divergence/convergence around the cloud is neglected, the total resistance is  $345 \Omega$ , highlighting the importance of the effect.

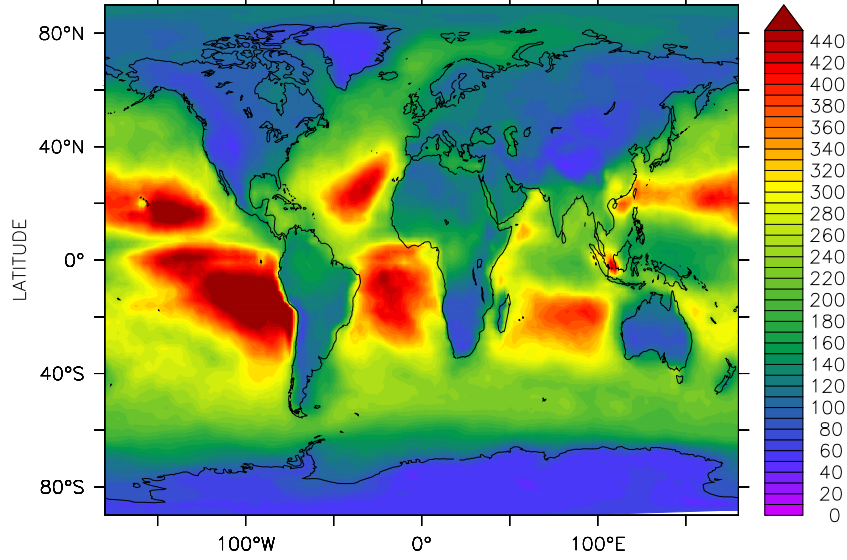


Figure 3: CESM1(WACCM) average column resistance ( $P\Omega m^2$ ).

### PARAMETRIZATION FOR 3-D CONDUCTIVITY CALCULATIONS

To account for the effect of non-electrified clouds in conductivity models with horizontal resolutions coarser than approx. 1 km, a parametrization is required. We introduce a correction to conductivity such that the vertical current assumption can be employed again, based on column resistance  $\tilde{R}_{col}$  from individual clouds simulations presented above. The model data required for this is the fair-weather column resistance and cloud cover fractions  $f(z)$  for every model grid cell. We define effective conductivity  $\tilde{\sigma}$  such that

$$\tilde{R}_{col} = \int \frac{dz}{\tilde{\sigma}(z)}. \quad (12)$$

and assume the following relationship between  $\tilde{\sigma}$  and the cloud-free conductivity:

$$\tilde{\sigma}(z) = (1 - f(z))\sigma(z) + \gamma f(z)\sigma(z) \quad (13)$$

where a parameter  $\gamma$  is introduced that will take into account the non-linearity introduced by the current divergence/convergence around the clouds. Using the assumed form for  $\tilde{\sigma}$  from Eq. 13, we can rewrite Eq. 12 as

$$\tilde{R}_{col} = \sum_{i=1}^n \frac{\Delta z}{\sigma(z)(1 - f(z)(1 - \gamma))} \quad (14)$$

for  $n$  model layers with thickness  $\Delta z$ . Eq. 14 is a polynomial with degree  $n$  for the variable  $\gamma$ . Here, Newton's method is used to numerically approximate  $\gamma$  for the function  $h(\gamma) = R - \sum \Delta z / (\sigma(1 - f(1 - \gamma))) = 0$ . The first derivative is  $h'(\gamma) = \sum \Delta z \sigma f / (\sigma(1 - f(1 - \gamma)))^2$ . With this, the solution is iteratively approximated using  $\gamma_{m+1} = \gamma_m - h(\gamma_m) / h'(\gamma_m)$ .

While the polynomial in general has  $n$  number of solutions, only the largest  $\gamma$  is physically meaningful. For other solutions conductivity of the layer with the largest cloud cover  $f$  becomes negative. The initial guess  $\gamma_0$  for the largest  $\gamma$  is close to where the fraction reaches singularity,  $\gamma_0 = 1 - 1/\max(f) + \epsilon$ . Then, Newton's method reliably converges to this solution. With  $\gamma$  from Eq. 13,  $\tilde{\sigma}(z)$  can then be calculated.

The effective conductivity distribution,  $\tilde{\sigma}$ , can be used for global GEC models to calculate potentials and currents, while accounting for sub-grid scale effects of non-electrified clouds.

## CONCLUSIONS

Using high-resolution model simulations that solve the Poisson type PDE for current flow in the fair-weather region of the GEC, the role of non-electrified clouds was investigated. A finite element model for the GEC was used to solve for potential and current in the vicinity of various cloud sizes and altitudes. Non-electrified clouds, which decrease electrical conductivity, in general, lead to a reduced current density beneath the cloud layer; however, the model shows that currents bend around the cloud, with current divergence above the cloud and convergence below. Below the cloud, this leads to larger current densities and effectively a smaller cloud resistivity than expected if only vertical currents were considered.

Using the Earth System Model CESM1(WACCM), non-electrified clouds were found to increase global resistance by up to  $120\ \Omega$  (73% of the cloud-free atmosphere resistance). A parametrization was developed that corrects conductivity depending on model grid cell cloud cover, allowing to assume only vertical current flow on the scale of grid columns.

**ACKNOWLEDGMENTS:** This work was supported by NSF Award AGS-1135446 to the University of Colorado under the Frontiers in Earth System Dynamics Program (FESD). We would like to acknowledge high-performance computing support from UCAR/Yellowstone.

## References

- Baumgaertner, A. J. G., J. P. Thayer, R. R. Neely, and G. Lucas, Toward a comprehensive global electric circuit model: Atmospheric conductivity and its variability in CESM1(WACCM) model simulations, *J. Geophys. Res.*, *118*, 9221–9232, 2013.
- Baumgaertner, A. J. G., G. M. Lucas, J. P. Thayer, and S. A. Mallios, On the role of non-electrified clouds in the global electric circuit, *Atmos. Chem. Phys. Discuss.*, *submitted*, 2014.
- Lamarque, J.-F., et al., CAM-chem: description and evaluation of interactive atmospheric chemistry in the Community Earth System Model, *Geosci. Model Dev.*, *5*, 369–411, 2012.
- Logg, A., K.-A. Mardal, G. N. Wells, et al., *Automated Solution of Differential Equations by the Finite Element Method*, Springer, 2012.
- Marsh, D. R., M. J. Mills, D. E. Kinnison, J.-F. Lamarque, N. Calvo, and L. M. Polvani, Climate Change from 1850 to 2005 Simulated in CESM1(WACCM), *J. Climate*, *26*, 7372–7391, 2013.
- Nicoll, K. A., and R. G. Harrison, Vertical current flow through extensive layer clouds, *J. Atmos. Sol-Terr. Phys.*, *71*, 2040–2046, 2009.
- Nicoll, K. A., and R. G. Harrison, Experimental determination of layer cloud edge charging from cosmic ray ionisation, *Geophys. Res. Lett.*, *37*, 13,802, 2010.
- Pruppacher, H. R., and J. D. Klett, *Microphysics of Clouds and Precipitation*, 2nd ed., Kluwer, 1997.
- Rycroft, M. J., R. G. Harrison, K. A. Nicoll, and E. A. Mareev, An Overview of Earth's Global Electric Circuit and Atmospheric Conductivity, *Space Science Rev.*, *137*, 83–105, 2008.
- Tinsley, B. A., and L. Zhou, Initial results of a global circuit model with variable stratospheric and tropospheric aerosols, *J. Geophys. Res.*, *111*, 16,205, 2006.
- Wood, R., and P. R. Field, The Distribution of Cloud Horizontal Sizes, *J. Climate*, *24*, 4800–4816, 2011.
- Zhou, L., and B. A. Tinsley, Production of space charge at the boundaries of layer clouds, *J. Geophys. Res.*, *112*, 11,203, 2007.
- Zhou, L., and B. A. Tinsley, Global Circuit Model with Clouds, *J. Atmos. Sci.*, *67*, 1143–1156, 2010.
- Zhou, L., and B. A. Tinsley, Time dependent charging of layer clouds in the global electric circuit, *Adv. Space Res.*, *50*, 828–842, 2012.